Chapter 7

The $\tan\beta - M_{H^\pm}$ bound from inclusive semi-tauonic B-decays in the MSSM

In this chapter we will compute the $\mathcal{O}(\alpha_s)$ SUSY-QCD and the leading SUSY-EW corrections to the W and charged Higgs mediated inclusive semi-tauonic B-decay, $\bar{B} \to \tau\,\bar{\nu}_\tau\,X$. Combining the SUSY contribution with the SM result obtained from the heavy quark effective field theory, plus ordinary QCD corrections, we find that the allowed region in the $(\tan\beta, M_{H^\pm})$-plane could be significantly modified by the short-distance supersymmetric effects. Since the sensitivity to the SUSY parameters other than μ (the higgsino mixing mass) is rather low, the following effective bound emerges for $\mu < 0$ at the $2\,\sigma$ level: $\tan\beta \lesssim 0.43\ \ (M_{H^\pm}/\,\mathrm{GeV})$. Remarkably, for $\mu > 0$ there could be no bound at all. Finally, we provide a combined $(\tan\beta, M_{H^\pm})$ exclusion plot using our B-meson results together with the recent data from top quark decays.

7.1 Motivation and experimental situation

Low-energy meson phenomenology can be a serious competitor to high energy physics in the search for extensions of the Standard Model (SM) of the strong and electroweak inter-

actions, such as general two-Higgs-doublet models (2HDM's) and Supersymmetry (SUSY). The simplest and most popular realization of the latter is the Minimal Supersymmetric Standard Model [17, 18]. At present, the potential manifestations of the MSSM are object of a systematic investigation. In this respect, B-meson physics has been doing an excellent job. On the one hand, the restrictions placed by radiative B^0 decays $\bar{B}^0 \to X_s\,\gamma$ (i.e. $b \to s\,\gamma$) on the global fit analyses [183] to indirect precision electroweak data have played a fundamental role. In the absence of SUSY, $b \to s\,\gamma$ alone is able to preclude general Type II 2HDM's involving charged Higgs masses $M_{H^\pm} \lesssim 150\,GeV$ [184, 185] as explained in Sec. 6.2. In fact, it is known that charged Higgs bosons of $\mathcal{O}(100)\,GeV$ interfere constructively with the SM amplitude of $b \to s\,\gamma$ and render a final value of $BR(b \to s\,\gamma)$ exceedingly high. This situation can be remedied in the MSSM –as seen in Sec.4.2.1– where there may be a compensating contribution from relatively light charginos and stops which tend to cancel the Higgs effects [122–129].

Thus, in the MSSM, the top quark decay $t \to H^+\,b$ may well be open and could be a clue to "virtual SUSY" [46].

On the other hand, semileptonic B-meson decays can also reveal themselves as an invaluable probe for new physics. In the specific case of the inclusive semi-tauonic B-meson decays, $B^- \to \tau^-\,\bar{\nu}_\tau\,X$, one defines the following ratio of rates

$$R = \frac{\Gamma(B^- \to \tau^-\,\bar{\nu}_\tau\,X)}{\Gamma(B^- \to l^-\,\bar{\nu}_l\,X)}\,, \tag{7.1}$$

where $l = e, \mu$ is a light lepton. The SM prediction of this ratio (see later on) is a bit lower than the average experimental measurements. The discrepancy is not dramatic, but it can be used to foster or, alternatively, to hamper particular extensions of the SM and, therefore, to restrict or even rule out certain non-SM domains of the extended parameter space where this "R anomaly" would aggravate. For example, the observable (7.1) is sensitive to two basic parameters of generic (Type II) 2HDM's, namely the ratio of VEV's, $\tan\beta = v_2/v_1$, and the (charged) Higgs mass, $M_H \equiv M_{H^\pm}$. As a consequence, the following upper bound at $1\,\sigma$ (resp. $2\,\sigma$) is claimed in the literature [53]:

$$\tan\beta < 0.49\ (0.52)\ \ (M_H\,/\,\mathrm{GeV})\,. \tag{7.2}$$

To derive this bound, use is made of previous LEP 1 data on semi-tauonic B-decays [186, 187]

$$BR(B^- \to \tau^- \bar{\nu}_\tau X) = (2.69 \pm 0.44)\% , \tag{7.3}$$

as well as of the former world average on semi-leptonic B-decays [188, 189]

$$BR(B^- \to l^- \bar{\nu}_l X) = (10.43 \pm 0.24)\% . \tag{7.4}$$

The bound (7.2) also hinges on the transition from the free quark model decay amplitude to the meson decay amplitude, as follows. At the quark level, the dominant contribution to $B^- \to \tau^- \bar{\nu}_\tau X$ comes from the exclusive quark decay $b \to \tau^- \bar{\nu}_\tau c$ computed within the framework of the spectator model. The latter works reasonably well for B mesons, since the energy release in the b-c transition is well above $\Lambda_{\rm QCD}$ and the typical hadronic scales ($\sim 1 GeV$). The next step in accuracy is to correct it for long-distance non-perturbative effects. In the presence of a heavy quark, such as the bottom quark, the leading non-perturbative corrections can be tailored with a QCD-based operator product expansion in powers of $1/m_b$ within the context of the heavy quark effective theory (HQET) [1]. This method has been worked out in detail in Ref. [192–194] to account for the semi-tauonic B- meson decays, and we refer the reader to these references for more information. Furthermore, hard gluon exchange can be as important as the HQET corrections, so that in general one has to include the $\mathcal{O}(\alpha_{\rm s})$ short-distance perturbative QCD effects, where $\alpha_{\rm s}(m_b) \simeq 0.22$. These effects have been evaluated in Refs. [192–196] for the standard (W-mediated) amplitude.

In 2HDM extensions of the SM, the previous analysis must be generalized to include the HQET-type and $\mathcal{O}(\alpha_{\rm s})$ QCD corrections from the H^--mediated amplitude (in interference with the W^- amplitude). These contributions have been computed in Refs. [53, 197], and the bound (7.2) was obtained. Notice that since the $\mathcal{O}(\alpha_{\rm s})$ corrections to the W-mediated amplitude cancel to a large extent in R, one would naturally expect that the relevant QCD corrections as far as the $\tan\beta - M_H$ bound is concerned should be those affecting the H-mediated amplitude for the semi-tauonic B-decay. Notwithstanding, in practice even this radiative effect is not too dramatic [53], at least for the ordinary QCD corrections.

[1] See e.g. Ref. [190, 191] for a detailed review of the HQET methods.

The bound (7.2) is usually considered as very strong, for there are no additional tree-level contributions to $B^- \to \tau^- \bar{\nu}_\tau X$ aside from W^- and H^- exchange. In particular, there are no tree-level exchange of SUSY particles (sparticles) in the MSSM. For this reason, the upper limit (7.2) is usually believed to be essentially model-independent; and at face value one would immediately translate it to the MSSM Higgs sector by arguing that the one-loop SUSY effects are at least as tiny as the ordinary QCD corrections. Remarkably enough, however, this turns out *not* to be the case in general, as we shall show by explicitly computing the supersymmetric short-distance QCD corrections (SUSY-QCD), which are expected to be here the leading SUSY effects also [46]. As a result, we will find that quantum effects in the MSSM should most likely amount to a more restrictive bound. In some cases, though, the bound can be more relaxed, and even evanesce.

To the best of our knowledge, the potential impact of SUSY quantum effects on semi-tauonic B-meson decays has not been assessed in the literature. However, we expect (see below) that one-loop gluino exchange can be very important; and, indeed, we find that the bound (7.2) is not as model-independent as originally thought. It may become significantly renormalized in the MSSM, where it has to be rephrased in a more complicated way as a function of the SUSY parameters

$$(\tan\beta, M_H, \mu, m_{\tilde{g}}, m_{\tilde{q}})\,, \tag{7.5}$$

where μ is the higgsino mixing parameter, $m_{\tilde{g}}$ is the gluino mass and $m_{\tilde{q}}$ are the scharm and sbottom masses ($\tilde{q} = \tilde{c}, \tilde{b}$).

7.2 The semileptonic B-decays at one loop in the MSSM

To evaluate the quantum corrections, we shall adopt the on-shell renormalization scheme (Sec 3.2). Apart from the standard interactions mediated by the weak gauge bosons, the Yukawa type Lagrangian describing the charged Higgs interactions between b and c quarks in the MSSM reads as follows:

$$\mathcal{L}_{Hcb} = \frac{g\,V_{cb}}{\sqrt{2}M_W}\, H^+\,\bar{c}\,[m_b \tan\beta\, P_R + m_c \cot\beta\, P_L]\, b + \text{h.c.}\,, \tag{7.6}$$

where $P_{L,R} = 1/2(1 \mp \gamma_5)$ are the chiral projector operators and $V_{cb} \simeq 0.04$ is the corresponding CKM matrix element. This matrix element cancels out in our analysis since we shall be concerned with the ratio (7.1).

The relevant supersymmetric parameters (7.5) for our analysis are contained in the SUSY-QCD Lagrangian [17, 18] and in the scharm and sbottom mass matrices eq. 2.26. Since $\tilde{c}$ and $\tilde{b}$ squarks belong to different weak-isospin multiplets, there is no $SU(2)$ correlation between the soft SUSY-breaking parameters in the two mass matrices.

Diagonalization of $\mathcal{M}^2_{\tilde{q}}$ is performed by independent rotation 2×2 matrices, $R^{(\tilde{q})}$. We will denote by $m_{\tilde{c}_1}$ ($m_{\tilde{b}_1}$) the lightest scharm (sbottom) mass-eigenvalues. For the sake of simplicity, we treat the two $R^{(\tilde{q})}$ assuming that the mixing angles are $\pi/4$. This is no loss of generality, since the feature of $\mathcal{M}^2_{\tilde{q}}$ that really matters for our calculation is that the off-diagonal element of the sbottom mass matrix is non-vanishing, so that at high $\tan\beta$ it behaves like $m_b\, M^b_{\rm LR} \simeq -\mu\ m_b \tan\beta$. The scharm mixing matrix, instead, is basically diagonal, for $m_c/m_{\tilde{c}_1} \ll 1$ and $M^c_{\rm LR}$ is not $\tan\beta$-enhanced.

The various contributions to the decay rate $\Gamma(B^- \to \tau^- \bar{\nu}_\tau\, X)$ are expressed as follows:

$$\Gamma_{\rm B} = \Gamma_{\rm HQET} + \delta\Gamma_{\rm W,H} + \delta\Gamma_{\rm I}\,. \tag{7.7}$$

Here $\Gamma_{\rm HQET}$ is the contribution from the HQET-corrected amplitudes mediated by W^-, H^- and interference terms at the tree-level, and $\delta\Gamma_{\rm W,H,I}$ are the short-distance QCD and SUSY-QCD corrections. For the semileptonic B-decay rate, $\Gamma(B^- \to l^-\, \bar{\nu}_l\, X)$, we have a similar formula (7.7) but we neglect all effects related to Higgs and interference terms.

The HQET corrections depend on a set of parameters $(\bar{\Lambda}, \lambda_1, \lambda_2)$ that connect the B and D meson masses to the bottom and charm quark masses [190–194]:

$$\begin{aligned} m_B &= m_b + \bar{\Lambda} - \frac{\lambda_1 + 3\,\lambda_2}{2\,m_b} + \ldots\,, \\ m_D &= m_c + \bar{\Lambda} - \frac{\lambda_1 + 3\,\lambda_2}{2\,m_c} + \ldots\,. \end{aligned} \tag{7.8}$$

This correlation between the pole masses m_c and m_b is one of the main improvements with respect to the spectator model. The explicit form for $\Gamma_{\rm HQET}$ as a function of these parameters is provided in Refs. [192–194, 197]. Fortunately, the standard QCD and SUSY-QCD

contributions to $\delta\Gamma_{\rm W}$ can also be extracted from the literature [110, 192–196] and cancel to a large extent[2] in the ratio (7.1).

Of special relevance are the QCD and SUSY-QCD contributions to the Higgs and interference terms, $\delta\Gamma_{\rm H,I}$. They can be computed using the framework of Refs. [40, 53, 165]. After a straightforward calculation, we arrive at the following formulae:

$$\begin{aligned}
\delta\Gamma_{\rm H} &= K \int_{\rho_\tau}^{(1-\sqrt{\rho_c})^2} dt \;\; H(t) \left(1-\frac{\rho_\tau}{t}\right)^2 \frac{t\,\rho_\tau\,\tan^2\beta}{\xi^2}\,(\delta a+\delta b)\,, \\
\delta\Gamma_{\rm I} &= -K \int_{\rho_\tau}^{(1-\sqrt{\rho_c})^2} dt \;\; I(t) \left(1-\frac{\rho_\tau}{t}\right)^2 \frac{\rho_\tau}{\xi}\,[\,\delta a+\delta b+\sqrt{\rho_c}\,(\delta a-\delta b)\,]\,,
\end{aligned} \tag{7.9}$$

with

$$K=\frac{G_F\,m_b^2\,\tan^2\beta}{4\sqrt{2}\,\pi^2}\,, \quad \rho_c=m_c^2/m_b^2\,, \quad \rho_\tau=m_\tau^2/m_b^2\,, \quad \xi=M_H^2/m_b^2\,. \tag{7.10}$$

We have introduced

$$H(t)=\Gamma_{\rm bcS}(\rho_c,t;2,0,1)\,, \qquad I(t)=\Gamma_{\rm bcS}(\rho_c,t;2,-2\sqrt{\rho_c},1)\,, \tag{7.11}$$

where $\Gamma_{\rm bcS}(\rho_c,t;c_1,c_2,c_3)$ is an appropriate (tree-level) function defined in Ref. [53]; it is related to the decay rate $b\to cS$ into a virtual scalar $S=H^-,G^-$. Here G^- is a Goldstone boson contribution, for the calculation is carried out in the convenient setting of the Landau gauge. Furthermore, $\delta a,\delta b$ in eq.(7.9) contain the ordinary QCD plus SUSY-QCD corrections to the effective couplings $a=a_H+a_G$ and $b=b_H+b_G$ standing in the interaction Lagrangian of S with charm and bottom quarks:

$$\frac{i\,g\,m_b\,\tan\beta\,V_{cb}}{2\sqrt{2}\,M_W}\,\bar{c}(a+b\,\gamma_5)\,b\,S\,. \tag{7.12}$$

7.2.1 The QCD and $\widetilde{\rm QCD}$ corrections

The standard QCD corrections $\delta a^{\rm QCD}$ and $\delta b^{\rm QCD}$ can be obtained by adapting the results of Ref. [165] whereas the SUSY-QCD corrections follow after straightforward modification of

[2] The SUSY-QCD corrections to the W-mediated amplitude can be derived from the work of Ref. [110]. They not only partially cancel out in the ratio R, but are rather small by themselves, namely of $\mathcal{O}(1)\%$. In contrast, the ordinary QCD corrections [192–196] are of $\mathcal{O}(10)\%$ but cancel in R to within $\mathcal{O}(1)\%$.

the form factors G_L, G_R of Sec. 4.4:

$$\delta a^{\rm SUSY-QCD} = G_R + \frac{\sqrt{\rho_c}}{\tan^2\beta}\, G_L\,,$$
$$\delta b^{\rm SUSY-QCD} = G_R - \frac{\sqrt{\rho_c}}{\tan^2\beta}\, G_L\,. \qquad (7.13)$$

In the limit of large $\tan\beta$,

$$\delta a^{\rm SUSY-QCD} \simeq\ \delta b^{\rm SUSY-QCD} \simeq\ G_R = H_R + \frac{\delta m_b}{m_b} + \frac{1}{2}\,\delta Z_L^c + \frac{1}{2}\,\delta Z_R^b\,, \qquad (7.14)$$

where H_R is a vertex form factor given by eq. 4.54 and the remaining terms are suitable mass and wave-function renormalization counterterms in the on-shell scheme (Sec. 4.4.3).

7.2.2 The $\widetilde{\rm EW}$ leading corrections

We will show also the effects of the leading $\widetilde{\rm EW}$ effects originating from the counterterm contribution $\frac{\delta m_b}{m_b}$, eq. 4.73:

$$\begin{aligned}\delta a^{\rm SUSY-EW} &\simeq \delta b^{\rm SUSY-EW} \simeq\ G_R \\ &\approx \frac{\delta m_b}{m_b} \simeq -\frac{h_t\, h_b}{16\pi^2}\,\frac{\mu}{m_b}\, m_t\, M_{LR}^t I(m_{\tilde{t}_1}, m_{\tilde{t}_2}, \mu) \\ &\to -\frac{h_t^2}{16\pi^2}\,\mu\tan\beta\, A_t\, I(m_{\tilde{t}_1}, m_{\tilde{t}_2}, \mu)\,, \end{aligned} \qquad (7.15)$$

7.3 Numerical Analysis

Collecting all the pieces from the RHS of eq.(7.7), we may now perform the numerical analysis of the ratio R – Cf. Figs. 7.1-7.4 and Table 7.1. We fix the error bars for the HQET parameters as in Ref. [53]; and to account for the uncertainties associated to $\mathcal{O}(\alpha_{\rm s}^2)$ corrections, we have also varied the renormalization scale such that $0.20 \leq \alpha_{\rm s} \leq 0.36$. As a first step in our numerical analysis (Cf. Figs. 7.1a and 7.4), we have carefully checked that we are able to recover the non-supersymmetric results [53, 192–194, 197]. Indeed, upon disconnecting the SUSY terms, we have verified (with the help of MINUIT) that we accurately reproduce the numerical results obtained for R as a function of $r \equiv \tan\beta/M_H$ (Cf. Fig. 1 of Ref. [53]); in particular, we recover the bound (7.2) based on the inputs (7.3)-(7.4).

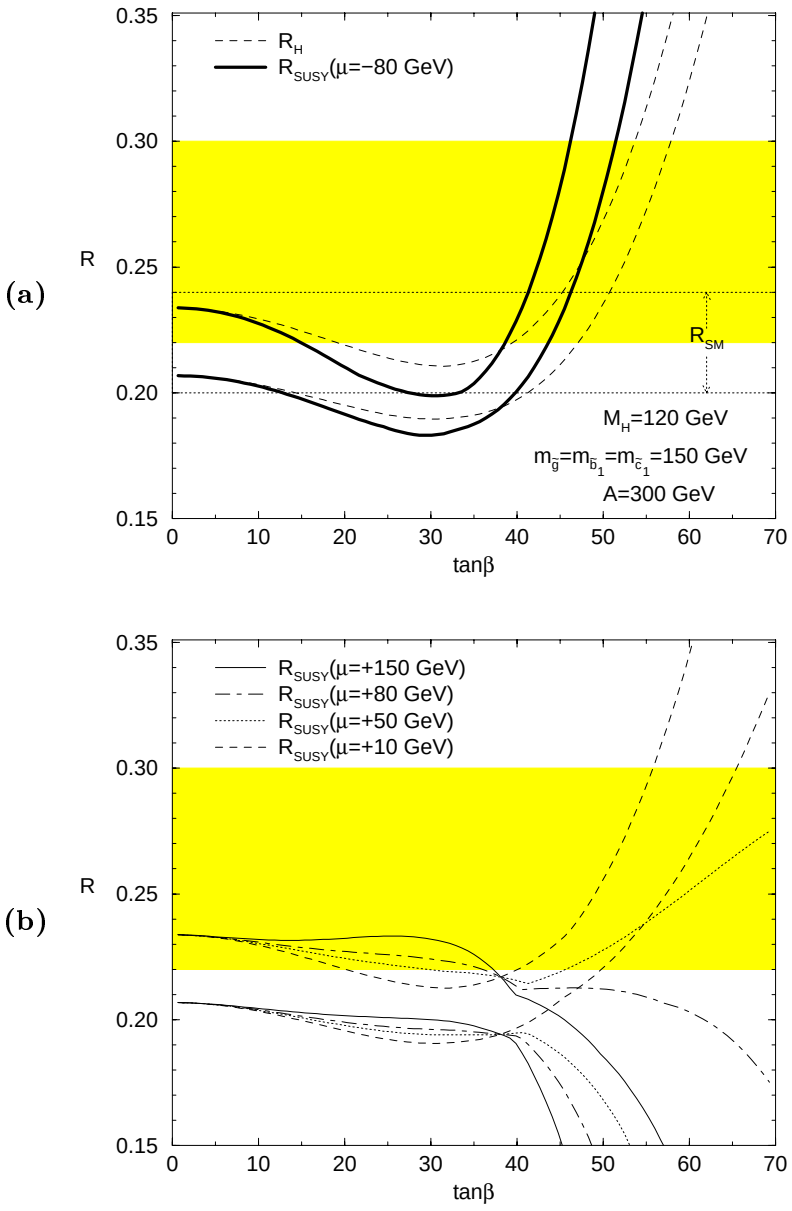

Figure 7.1: **(a)** *The SUSY-QCD corrected ratio R_{SUSY}, eq.(7.1), as a function of* $\tan\beta$*, for $\mu = -80\,GeV$ and given values of the other parameters (7.5). The HQET and* α_s *parameter ranges are as in Ref. [53]. Also shown are the SM result, R_{SM}, (dotted band) and the Higgs-corrected result without SUSY effects, R_H. The shaded band is the experimental measurement at the $1\,\sigma$ level as given by eqs.(7.3)-(7.4);* **(b)** *As in (a), but for $\mu = +10, +50, +80, +150\,GeV$.*

	$\mu\ (GeV)$	$m_{\tilde{g}}\ (GeV)$	$m_{\tilde{b}_1}\ (GeV)$	$r_{max}\ (GeV^{-1})\ 1\sigma\ (2\sigma)$	
				(i)	(ii)
A	-80	150	150	0.42 (0.44)	0.40 (0.43)
B	-80	150	300	0.45 (0.47)	0.43 (0.45)
C	-150	300	300	0.42 (0.44)	0.40 (0.42)
D	-300	400	400	0.40 (0.42)	0.39 (0.41)

Table 7.1: *Effective* $\tan\beta/M_H < r_{\rm max}$ *bound for four* $\mu < 0$ *scenarios: A) corresponds to the (approximate) present day mass limits on sparticles; B) is defined by the combination of sparticle masses giving the worst possible bound on* $r_{\rm max}$*; finally, C,D) reflect the situation for future sparticle mass limits. In the four cases, we show the* $1\,\sigma$ *(*$2\,\sigma$*) upper bounds on* $r_{\rm max}$ *for the two sets of inputs: (i) eqs.(7.3)-(7.4) and (ii) eqs.(7.16)-(7.17).*

At present, the experimental situation has changed a little. For example, a recent ALEPH measurement yields [198–200]

$$BR(B^- \to \tau^-\,\bar{\nu}_\tau\,X) = (2.72 \pm 0.34)\%\,, \tag{7.16}$$

which is slightly more tight[3]. However, also the inclusive semileptonic branching ratio has changed slightly. On the one hand, the LEP electroweak working group uses

$$BR(B^- \to l^-\,\bar{\nu}_l\,X) = (11.2 \pm 0.4)\%\,, \tag{7.17}$$

and on the other hand the CLEO/ARGUS and L3 results suggest a lower value which brings the average closer to (7.4). In view of this situation, and since we wish to make clear that our SUSY effects are potentially "real", i.e. that they are not just an artifact associated to the change of the experimental inputs, we shall first of all normalize our analysis with respect to the same inputs (7.3)-(7.4) used in Ref. [53] and thus present our results (Figs. 7.1-7.4) in this

[3]We point out the two experimental values since the older one, eq.(7.3), is an average of previous ALEPH and L3 measurements [186, 187], whilst the new one, eq.(7.16), is an average of measurements of only the ALEPH Collaboration based on two different experimental techniques [198–200].

framework. Notice that, in the SUSY case, the analysis cannot be strictly formulated in terms of the single parameter r, but rather as a function of $\tan\beta$, M_H and the rest of parameters (7.5). Still, limits on an effective r can be given after fully exploring the parameter space. These are given in Table 7.1, where we exhibit in a nutshell our final numerical results on the $\tan\beta - M_H$ bound. We reserve the last column of that table for the results obtained by using the most recent LEP data, i.e. eqs.(7.16)-(7.17). By this procedure we have fitted the relevant part of the physical boundary of the $(\tan\beta, M_H)$-space to the linear form $\tan\beta = r_{\max} M_H$, where $r_{\max}$ is the maximum "effective slope" compatible with the sparticle mass parameters given in Table 7.1. In this way we can easily compare our SUSY results with the general (Type II) 2HDM bound (7.2). It should be emphasized that a good local linear regression in the SUSY case is possible (Cf. Fig. 7.4) because the ratio R has low sensitivity to the squark and gluino masses in the few hundred GeV range, as it is borne out in Figs. 7.2a-7.2b – see further comments below.

In the following we analyze things in more detail. For fixed $M_H = 120\,GeV$, the plot of R, eq.(7.1), as a function of $\tan\beta$ is shown in Fig. 7.1a for $\mu < 0$ and in Fig. 7.1b for $\mu > 0$. The shaded region gives the experimental band at $1\,\sigma$ as determined from eqs.(7.3)-(7.4). The SUSY-QCD effects in Figs. 7.1a-7.1b are computed for the (approximate) present bounds on sparticle masses, namely $m_{\tilde{g}} = 150\,GeV$ and $m_{\tilde{b}_1} = m_{\tilde{c}_1} = 150\,GeV$ (Scenario A in Table 7.1). We have also fixed $A_c = A_b = 300\,GeV \equiv A$, but the dependence on this parameter is not important at high $\tan\beta$. A most interesting parameter is μ. It is plain from Figs. 7.1a-7.1b that both the sign and size of μ are material; indeed, the larger is $|\mu|$ (for $\mu < 0$) the steepest is the ascent of R into the experimental band and so the narrower is the preferred interval of high $\tan\beta$ values. On the contrary, for smaller and smaller $|\mu|$ the SUSY effect dies away. In all figures where a definite $\mu < 0$ is to be chosen, the value $\mu = -80\,GeV$ (Scenario A) is taken, except in Fig. 7.1b where the case $\mu > 0$ is addressed in detail. It is easy to see from the structure of the chargino mass matrix in the higgsino-gaugino variables [17, 18] that, in the high $\tan\beta > 10$ region, $\mu = -80\,GeV$ is the minimum allowed value of $|\mu|$ compatible with the LEP 1.61 phenomenological bound $m_{\chi_1^\pm} \gtrsim 80\,GeV$. The latter is the strongest phenomenological mass limit on charginos available from LEP,

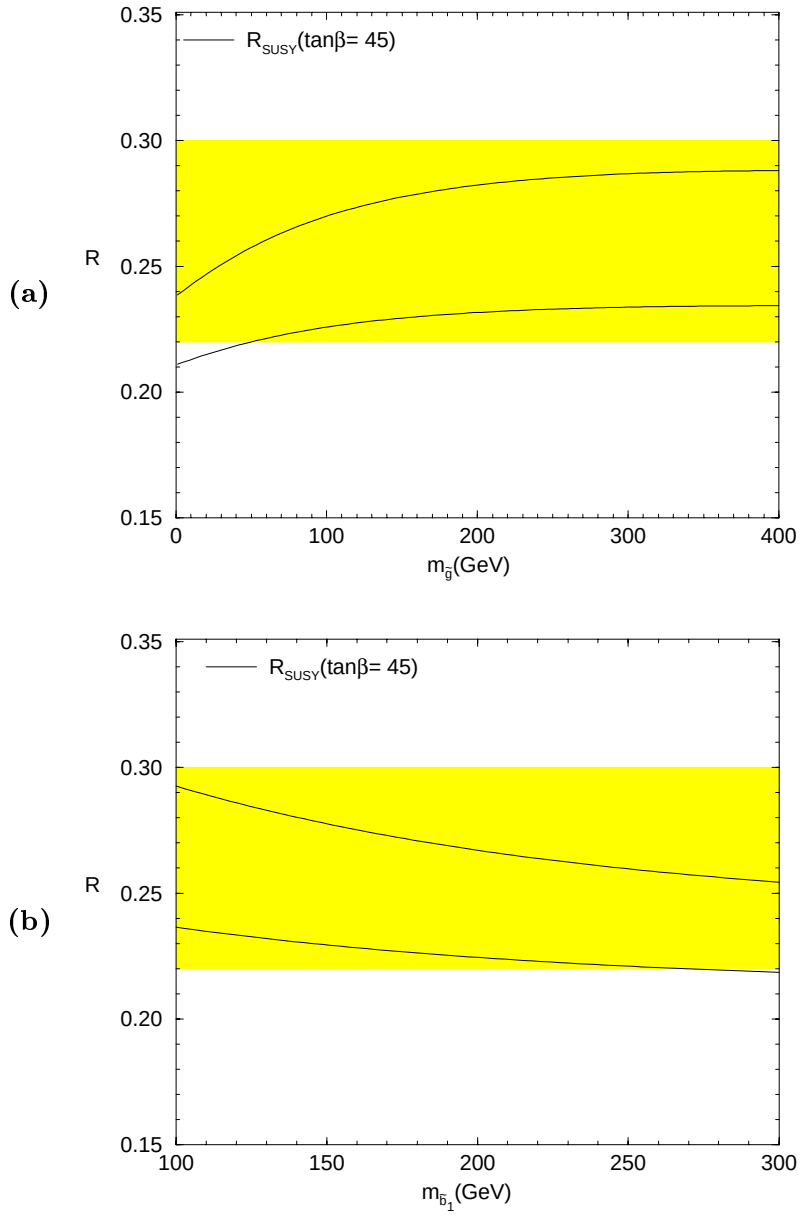

Figure 7.2: **(a)** *Dependence of* R_{SUSY} *upon the lightest sbottom mass for* $\tan\beta = 45$. *Remaining inputs as in Fig. 7.1a.* **(b)** R_{SUSY} *as a function of the gluino mass, and the rest of inputs as in (a).*

and corresponds to the so-called neutralino LSP scenario.

Due to the variation of the HQET parameters and α_s in the aforementioned ranges, our results are not single curves but " beam curves". For a better understanding, in Fig. 7.1a we have simultaneously plotted, as a function of $\tan\beta$, the beam curves for:

- (i) The fully SUSY-QCD corrected ratio R, eq.(7.1), which we call R_{SUSY}, including all effects present in eq.(7.7);

- (ii) The Higgs-corrected ratio R, denoted R_H, with HQET and ordinary QCD corrections but without SUSY-QCD effects;

- (ii) The ratio R without Higgs effects, i.e. the (so-called) standard model (SM) prediction, computed with only the W-mediated amplitude including HQET and ordinary QCD corrections. It is represented in Fig. 7.1a by the narrow dotted band defined by $R_{SM} = 0.22 \pm 0.02$.

From Fig. 7.1a it is patent that the SM prediction lies tangentially below the experimental range, specifically $1\,\sigma$ below the central value of the experimental band. Admittedly, this "R anomaly" is not that serious and varies a bit depending on the data set used. In any case a useful bound on multiple Higgs extensions of the SM can be derived. It is evident from Fig. 7.1a that charged Higgs effects go in the right direction; for they shift the theoretical result entirely into the experimental range, to the extent that R_H may even overshoot the upper experimental limit at sufficiently high $\tan\beta$. To prevent this from happening, the bound (7.2) must be imposed [53]. Similarly, if the charged Higgs is a SUSY Higgs, there are additional SUSY effects that may substantially alter the picture both quantitatively and qualitatively. Indeed, a most vivid SUSY impinge on R occurs for $\mu < 0$ which triggers a sudden "re-entering" of the theoretical ratio R_{SUSY} into the experimental band at an earlier value of $\tan\beta$ and for a sharper range than in the R_H case.

We point out that the sign $\mu > 0$, although it is not the most suited one for R (Cf. Fig. 7.1b), it cannot be convincingly excluded, and it may even hide some surprises. To start with, we observe that the $\mu > 0$ beam curves overlap with the SM band all the way up to

$\tan\beta \gtrsim 40$. Nevertheless, for $\tan\beta > 40$ the beams behave very differently, depending on the value of μ; to wit:

- i) If $\mu > 80 - 90\,GeV$, they quickly run away the experimental band from below;
- ii) If $\mu < 20\,GeV$, they bend back into the experimental range past the R_H limit;
- iii) Finally, if $20\,GeV \lesssim \mu \lesssim 80\,GeV$, they spread very widely, mainly because of the variation with α_s.

In the first case, $\mu > 0$ becomes excluded at very high $\tan\beta$; in the second case, the bound (7.2) is violated since larger values of $\tan\beta$ are allowed for a given M_H; and in the third case, remarkably enough, the beam curves (partly) overlap all the time with the experimental region until the perturbative limit $\tan\beta \lesssim 60$ is already met. Therefore, for $20\,GeV \lesssim \mu \lesssim 80\ GeV$ a dramatic qualitative change occurs: the bound is fully destroyed, i.e. at the $2\,\sigma$ level there is no bound at all!. However, small values of $|\mu|$ are not recommended by present LEP data, as advertised before, and in this sense $\mu > 0$ values in the previous interval might already be excluded by LEP.

From the point of view of the "R anomaly", the sign $\mu < 0$ becomes strongly preferred since, then, there always exists a high $\tan\beta$ interval where all the beam curves rush into the experimental band for any value of $|\mu|$. In this case, compatibility with $b \to s\,\gamma$ requires $A_t > 0$ [122–129] (see Sec. 4.2.1). Hence at present the combined status of neutral and charged B-meson decays points to the signs $\mu < 0$ and $A_t > 0$. This feature does not depend on the values of the other SUSY parameters (7.5), as it is confirmed in Figs. 7.2a-7.2b where we explore the dependencies on the sbottom and gluino masses for fixed $\tan\beta$. The evolution with $m_{\tilde{b}_1}$ shows a slow decoupling (Fig. 7.2a) while the dependence on $m_{\tilde{g}}$ is such that, locally, the SUSY-QCD corrections slightly increase with $m_{\tilde{g}}$ (Cf. Fig. 7.2b) and eventually decouple (not shown). However, the decoupling rate turns out to be so slow that one may reach $m_{\tilde{g}} \sim 1\,TeV$ without yet undergoing dramatic suppression. Finally, the evolution with the scharm masses is very mild and it is not displayed.

As explained in Sec. 4.4.4 the leading source of SUSY-QCD effects originates from a (finite) bottom mass renormalization effect in the form factor G_R (Sec. 4.4.4). Specifically,

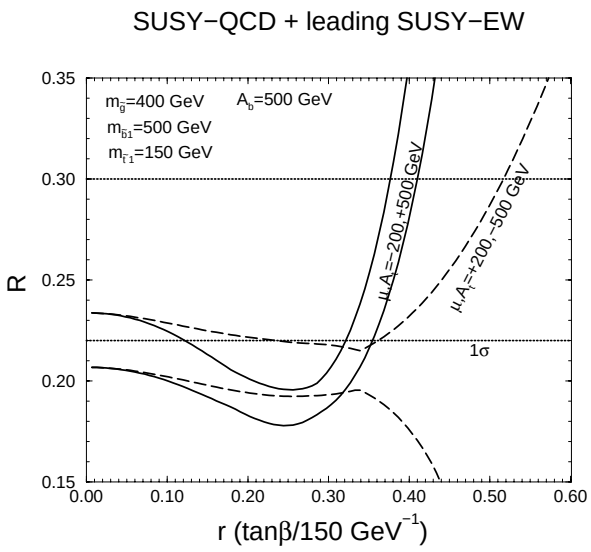

Figure 7.3: *The SUSY-QCD corrected ratio R_{SUSY}, eq.(7.1) when including the leading* $\widetilde{\text{EW}}$ *effects.*

this effect is contained in eq.(7.14) through eq. 4.71:

$$\begin{aligned}\left(\frac{\delta m_b}{m_b}\right)_{\text{SUSY-QCD}} &= C_F\,\frac{\alpha_s}{2\pi}\,m_{\tilde g}\,M^b_{LR}\,I(m_{\tilde b_1}, m_{\tilde b_2}, m_{\tilde g}) + ... \\ &\simeq -\frac{2\alpha_s}{3\pi}\,m_{\tilde g}\,\mu\tan\beta\,I(m_{\tilde b_1}, m_{\tilde b_2}, m_{\tilde g}) + ...\,,\end{aligned}$$

As an aside, we point out that the so-called light gluino scenario is not favoured in our case, since eq.(4.71) vanishes for $m_{\tilde g} = 0$.

The other potentially large $\tan\beta$ effect [129, 133, 134], the one due to chargino-stop diagrams, is typically smaller than the gluino diagram. Although it is true that for vanishing gluino mass it could dominate the large $\tan\beta$ effects, notice that the light gluino scenario is nowadays essentially dead. Recent LEP analyses do exclude light gluinos below $6.3\,GeV$ [201]. For gluino masses as in Table 7.1, compatibility with $b \to s\,\gamma$ (see below) renders that effect generally subleading. Nevertheless as shown in Fig. 7.3 for positive μ (which compels A_t to be negative) the effect is important and opens up this region, otherwise forbidden. In this case, the $\widetilde{\text{EW}}$ contributions are contrary in sign to the $\widetilde{\text{QCD}}$ ones.

In Fig. 7.4 we display the results of our analysis in the $(\tan\beta, M_H)$-plane for Scenario

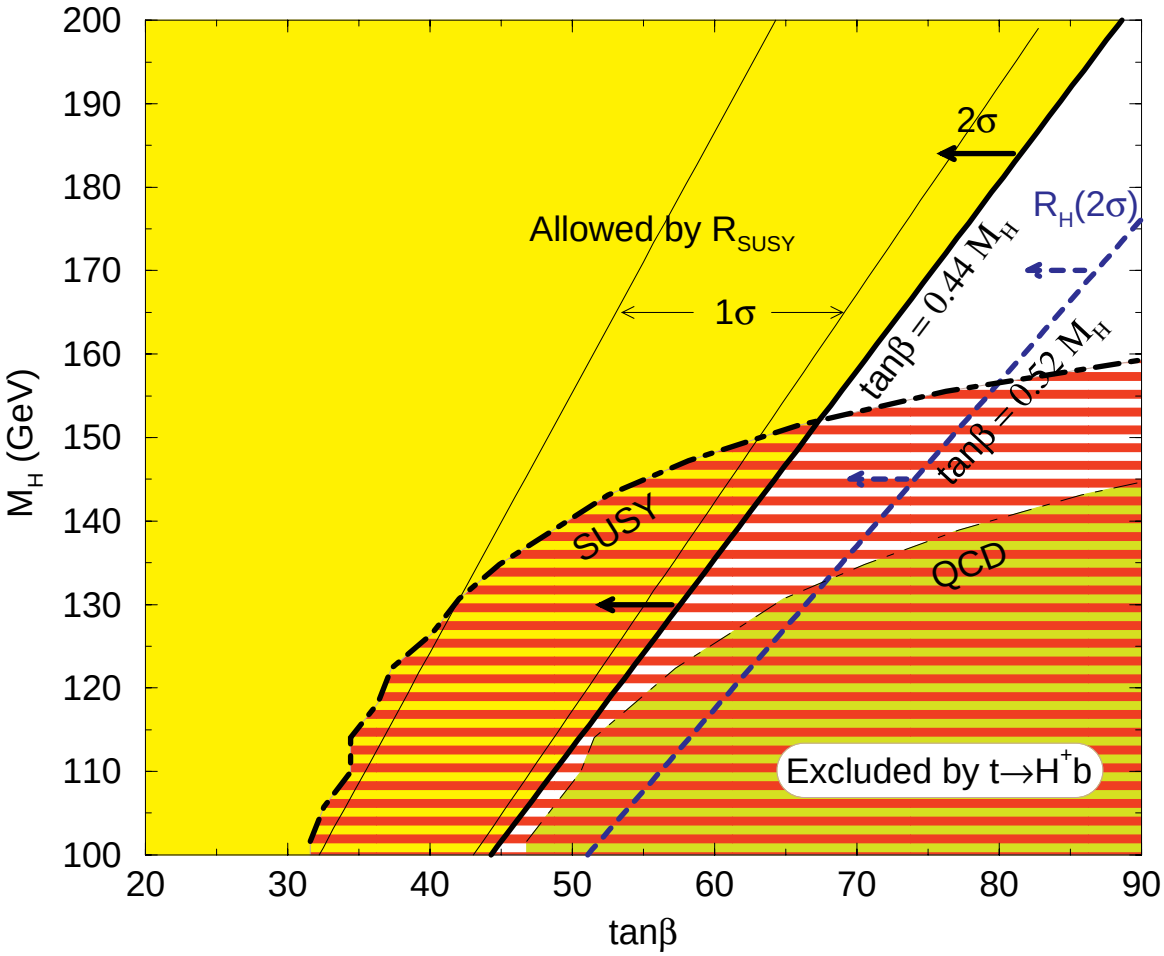

Figure 7.4: *Allowed region in the* $(\tan\beta, M_{H^\pm})$*-plane. Direct LEP limits on* M_{A^0} *already imply* $M_{H^\pm} \gtrsim 100\,GeV$ *in the MSSM. The shaded region limited by the bold solid line is allowed at the* $2\,\sigma$ *level by* R_{SUSY} *for the same fixed parameters as in Fig. 7.1a. The narrow subarea between the thin solid lines is permitted at* $1\,\sigma$ *only. (The larger is* $|\mu|$ *the narrower is this area.) In contrast, the allowed region at* $2\,\sigma$ *by the non-supersymmetric calculation,* R_H*, is the one placed above the dashed line. Also shown is the region excluded (at* $2\,\sigma$*) by the non-observation of* $t \to H^+\,b$ *at the Tevatron (including SUSY and just QCD effects).*

A and inputs (7.3)-(7.4). As stated, we concentrate on the case $\mu < 0$. Recall that, in the MSSM, the lowest allowed charged Higgs mass is $M_H \gtrsim 100\,GeV$ since it is correlated with the present LEP bound on the CP-odd Higgs mass, $M_{A^0} \gtrsim 60\,GeV$. At the $2\,\sigma$ level, the allowed region by the SUSY-corrected ratio R_{SUSY} is the big shaded area on the left upper part of Fig. 7.4. In contrast, at the $1\,\sigma$ level the permitted area is much smaller, and it is represented by that slice of the big shaded area limited by the two thin solid lines. Of course, lower segments of $\tan\beta$ are also allowed at $1\,\sigma$ but they do not entail any improvement at all with respect to the SM. Hence if we just concentrate on the high $\tan\beta > 30$ region, it turns out that at $1\,\sigma$ there exists only a narrow range of optimal $\tan\beta$ values for any given M_H. This was already evident from Fig. 7.1a where $M_H = 120\,GeV$. If we would now superimpose the perturbative limit ($\tan\beta \lesssim 60$) we would find that the highest allowed charged Higgs mass in Fig. 7.4 is rather small: $M_H < 190\,GeV$. At $2\,\sigma$, however, we have seen that the situation is far more permissive and one cannot place that bound; yet the allowed area by R_{SUSY} at $2\,\sigma$ is significantly smaller than the one allowed (at the same confidence level) by the non-supersymmetric ratio R_H (see dashed line in Fig. 7.4). A good linear approximation to the SUSY-corrected $2\,\sigma$ boundary is possible in the $(\tan\beta, M_H)$ window of Fig. 7.4. It corresponds to an "effective slope" of $r_{\rm max} = 0.44\,GeV^{-1}$.

From recent analysis [167, 177] of τ-lepton physics at the Tevatron, based on the *non*-observation of the decay $t \to H^+\,b$ followed by $H^+ \to \tau^+\,\nu_\tau$, it is possible to find a different (high-energy) exclusion plot in the $(\tan\beta, M_H)$-plane. The latter is represented, at the $2\,\sigma$ level, by the cross-hatched area in the low right corner of Fig. 7.4, where the QCD [177] and SUSY [167] corrected results are depicted. Interestingly enough, however, it turns out that the if we did not include the SUSY effects on the analysis of the τ-lepton physics at the Tevatron the excluded region of the $(\tan\beta, M_H)$-plane obtained from SUSY-corrected B-meson decays would be the most stringent one and basically would override the other exclusion plots, as can be appraised in Fig. 7.4.

Finally, we will show how this region changes when including the leading $\widetilde{\rm EW}$ quantum corrections for a case in which they are not completely subleading, that is when the $\widetilde{\rm QCD}$ corrections are small –as seen in sec. 4.4.4 this happens for large $m_{\tilde{b}_1}$. In this case $\widetilde{\rm QCD}$ and

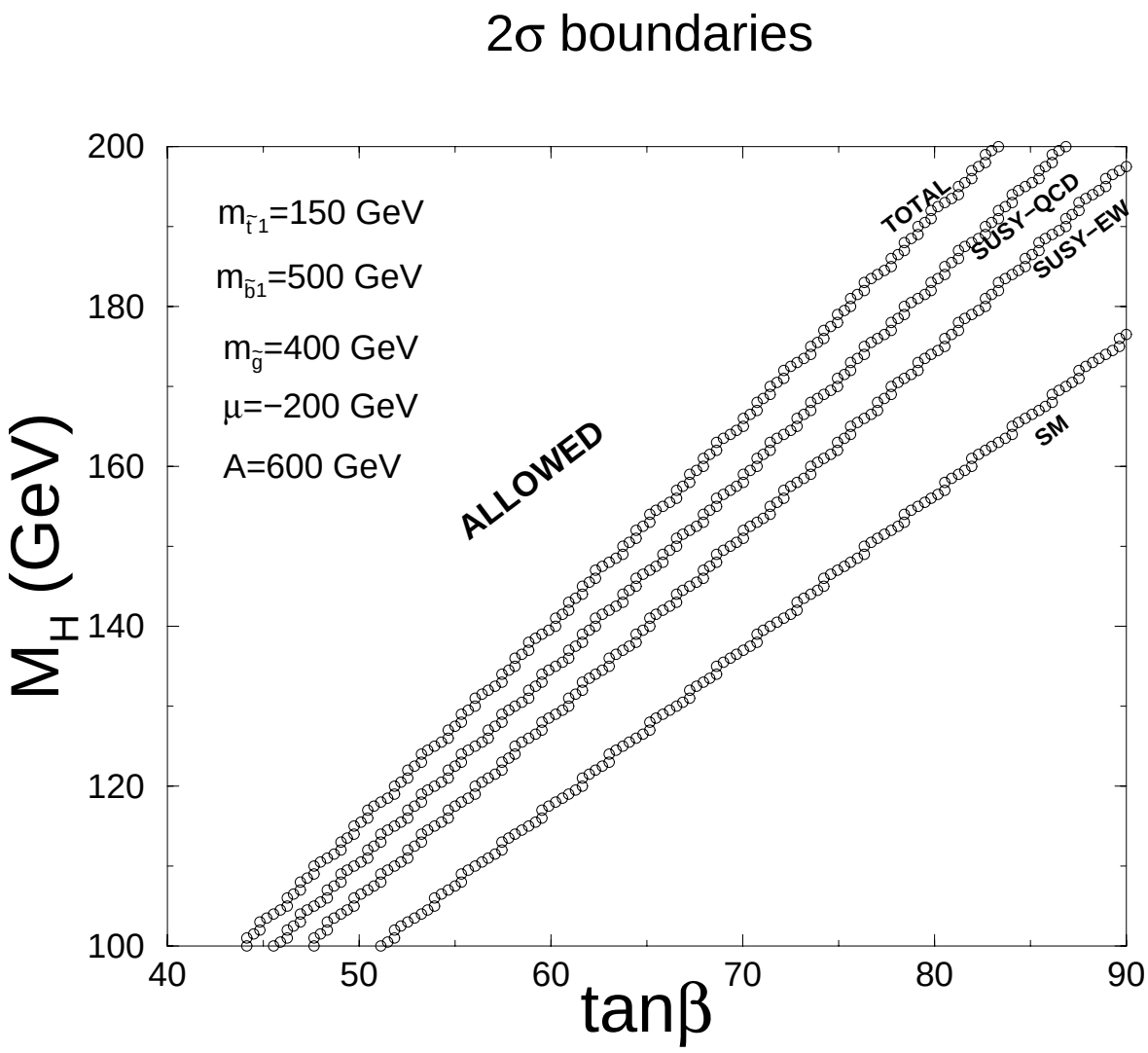

Figure 7.5: *Comparison of the allowed region in the* $(\tan\beta, M_{H^\pm})$*-plane when including only the* $\widetilde{\mathrm{QCD}}$ *effects, the leading* $\widetilde{\mathrm{EW}}$ *(eq. 7.15) ones and both (Total).*

$\widetilde{\mathrm{EW}}$ add up in sign and render a larger excluded area. It can be seen in Fig. 7.5, there we show the $\widetilde{\mathrm{QCD}}$ and $\widetilde{\mathrm{EW}}$ corrected cases and the "totally" corrected one. The corresponding restrictions at the 2σ level for the $\widetilde{\mathrm{QCD}}$ and $\widetilde{\mathrm{EW}}$ corrected case is:

$$\tan\beta < 0.39 \;\; (M_H \,/\, \mathrm{GeV})\,, \tag{7.18}$$

that should be compared with the jus $\widetilde{\mathrm{QCD}}$ corrected bound in this case:

$$\tan\beta < 0.41 \;\; (M_H \,/\, \mathrm{GeV})\,. \tag{7.19}$$

A final remark is in order. We have stated at the beginning that the decay $b \to s\,\gamma$ plays an important role in constraining the MSSM parameter space. Therefore, it is necessary to check explicitly the compatibility between the $b \to s\,\gamma$ constraints and the ones from semi-tauonic B-decays. This can most easily be performed using the eq. 4.4 (see Sec. 4.2.1)

$$BR(b \to s\,\gamma) \simeq BR(b \to c\,e\,\bar{\nu})\,\frac{(6\,\alpha_{\mathrm{em}}/\pi)\,\left(\eta^{16/23}\,A_\gamma + C\right)^2}{I(m_c/m_b)\,\left[1 - \frac{2}{3\pi}\,\alpha_{\mathrm{s}}(m_b) f_{\mathrm{QCD}}(m_c/m_b)\right]}$$

where $A_\gamma = A_{\mathrm{SM}} + A_{H^-} + A_{\chi^-}$ stands for the sum of the SM, charged Higgs and chargino-stop amplitudes, respectively. The contribution from a SUSY-QCD amplitude is in this case generally smaller. (Notice that when using eq.(4.4) one should make allowance for possible additional corrections of order 30% stemming from higher order QCD effects not included in it [122–129].)

The $b \to s\,\gamma$ consistency check is necessary because one may worry whether at large $\tan\beta$ (the regime that we have favoured in our study of semi-tauonic B-decays) and for sizable A_t the chargino amplitude might be enhanced and perhaps overshoot the CLEO bound [132] in the other direction, i.e. it could grow to the point of overcompensating the SM plus charged Higgs contribution. However, we have explicitly checked in all cases that upon using the same input parameters as in the present analysis, the CLEO bound can be respected. For definiteness in our presentation, we consider the following set of inputs: $M_{H^\pm} = 120\,GeV$, $\mu = -80\,GeV$ and $\tan\beta = 30 - 40$. We then find two possible types of solutions: namely, either the two stops are relatively heavy (roughly degenerate at about $300\,GeV$) and A_t remains bounded within any of the approximate intervals $(10, 60)\,GeV$ and $(100, 150)\,GeV$;

or another possibility is that one of the stops is relatively light (for example just above the present approximate LEP bound: $m_{\tilde{t}_1} > 65\,GeV$) and the other one is very heavy (we take it $m_{\tilde{t}_2} = 1\,TeV$). In this case A_t is forced to lie in the approximate intervals $(-400, -200)\,GeV$ and $(-100, +20)\,GeV$.

7.4 Conclusions

To summarize, we have assessed the impact of the SUSY-QCD and the leading $\widetilde{\mathrm{EW}}$ short-distance effects on the physics of the semi-tauonic inclusive B-meson decays within the framework of the MSSM. A regime of large $\tan\beta > 30$ is singled out. In this regime, the $\mu > 0$ case with $\mu > 80\,GeV$ would be ruled out if the $\widetilde{\mathrm{EW}}$ effects were not taken into account. On the other hand, for the most likely case $\mu < 0$, the SUSY effects further restrict the allowed region in the $(\tan\beta, M_H)$-plane as compared to eq.(7.2). A clear-cut résumé of our $\mu < 0$ results including just $\widetilde{\mathrm{QCD}}$ is conveniently displayed in Table 7.1. Using the present day sparticle mass limits and the recent LEP input data on B-meson decays – i.e. Scenario A (ii) in Table 7.1 – we have at the $1\,\sigma$ $(2\,\sigma)$ level:

$$\tan\beta < 0.40\ (0.43)\ \ (M_H\,/\,\mathrm{GeV})\,. \tag{7.20}$$

Since $M_H \geq 100\,GeV$ in the MSSM, it follows that the SUSY-QCD effects compel the maximum allowed value of $\tan\beta$ to be at least 9 units smaller than it was allowed by the previous bound, eq.(7.2), i.e. in general r receives a SUSY correction over -15%. We have also considered a situation (Scenario B) where gluinos are kept at the current phenomenological mass limit while the (lightest) sbottom is twice as much heavier than in Scenario A. This is the maximum conspiracy against our bound for these mass ranges, and yet the result for r_{max} varies less than 7%. Finally, C and D in Table 7.1 reflect future scenarios characterized by large squark and gluino masses as well as a substantially improved limit for the higgsino mass parameter. We wish to emphasize that, for $|\mu| \gtrsim 150\,GeV$, r_{max} is already essentially saturated in the value of $|\mu|$, i.e. larger values do not appreciably modify r_{max}. Notice that the leading effect (4.71) does not decouple when the masses of the sparticles involved in it are scaled up by keeping their ratios fixed. This is verified in Table 7.1 where we see that

scenarios A and C give essentially the same result.

If we add the leading $\widetilde{\mathrm{EW}}$ quantum corrections (eq. 4.73) we find that positive μ are indeed allowed and that for $\mu < 0$ the bound at the 2σ level, for an area in which we know the these effects to be comparable to the $\widetilde{\mathrm{QCD}}$ ones, is:

$$\tan\beta < 0.39 \ \ (M_H \,/\, \mathrm{GeV})\,,$$

Therefore, our results look fairly stable within the phenomenologically interesting portion of the parameter space (7.5) and should be considered as rather general in the context of the MSSM. We have also found that at present the information on the parameter space $(\tan\beta, M_H)$ as collected from B-meson decays is complementary to the one from top quark decays. Clearly, knowledge from both low-energy and high-energy data can be very useful to better pinpoint in the future the physical boundaries of the MSSM parameter space. Alternatively, if the two approaches would converge to a given portion of that parameter space, one could claim strong indirect evidence of SUSY.